Development of a Simple Correlation between the Mal Distribution Factor and Geometrical Parameters of the Two-Direction Vapor Horn Gas Distributor

Haojie Li[1], Bin Jiang[1], Ci Zhao[2], Luhong Zhang[1], Yongli Sun[1] and Xiaoming Xiao[1]

[1] *School of Chemical Engineering and Technology, No. 50 Building, Tianjin University, 135 Yaguan Road, Jinnan District, Tianjin 300072, People's Republic of China*
[2] *Chinese Research Academy of Environmental Science, No. 8 Dayangfang, Anwai Beiyuan, Chaoyang District, Beijing 100012, People's Republic of China*

Keywords: Distillation, CFD, Gas Distributor, Parameter Fitting, Two Direction Vapor Horn

Mal distribution and pressure drop are two important parameters for evaluating gas distributors, especially in vacuum towers. However, in many cases, the optimal results of these two parameters cannot be obtained simultaneously. To solve this problem, all the key geometric parameters of a two-direction vapor horn gas distributor were systematically analyzed in this study. These include the diameter of the column (*D*), inlet diameter (*d*), space between Inner sleeve and tower wall (*H*), height of inner sleeve (*h*), height of first vane (*h'*), radial slop angle (*θ*), number of vanes (*N*), inlet velocity in the column (*v*). The results showed that the pressure drop was mostly influenced by the space size at the inlet of the distributor, and the location of the high-speed zone of the gas was mainly affected by the gap between the inner sleeve and tower wall, height of the first vane, and number of vanes. Furthermore, an orthogonal experiment was conducted to obtain two correlation equations connecting the geometrically structured parameters with the pressure drop and mal distribution factor of the gas. This could help in predicting the gas distribution uniformity and pressure drop within the two-direction vapor horn gas distributor.

Introduction

As one of the efficient gas–liquid contacting devices, the structured packing towers have been widely used in industrial applications for decades. With the maturity of the packing-tower technology, large-scale packed towers have been gradually applied in rectification, absorption, and other unit operations. The development of high porosity, low pressure drop, and highly efficient packing further promoted the design and application of packing towers with a large diameter, shallow bed, and low liquid to gas ratio.

For the high vacuum–rectification process, the pressure drop within the gas inlet section should be small enough, considering the pressure drop for the tower is relatively small. In addition, the rapid uniform distribution of the gas into the tower is of vital importance as each segment comprises only 3–4 theoretical plates; otherwise, the separation efficiency of a packed tower is greatly reduced (Muir and Briens, 1986; Dhotre and Joshi, 2007; Haghshenasfard *et al.*, 2007; Venkatesh *et al.*, 2019). To achieve a better distribution effect, a more complex structure is required for the inlet devices; however, this inevitably leads to a greater pressure drop. This implies that the small pressure drop and good distribution of gas are contradictory in many cases in the operation of the distributor. Consequently, to make a trade-off between pressure drop and uniformity, the influence of the various geometric parameters for the design of the distributor must be quantitatively analyzed.

With the increasing industrial demands for highly uniform and low-pressure-drop inlet devices, a growing number of novel distributors have been studied over decades. Muir and Briens (1986) experimentally studied the effect of different feeding modes on the gas distribution. They found that that annular distribution plate could significantly improve gas distribution. Haghshenasfard *et al.* (2007) proposed the low Reynolds *k*-epsilon model to simulate the fluid flow within several gas inlet devices, including straight, sloped and bend inlets, and achieved good agreement between simulation data and experimental results. Dhotre and Joshi (2007) simulated the flow pattern on the upstream and downstream of distributor and evaluated its effect on performance of bubble column. Venkatesh *et al.* (2019) optimized the bottom inlet cyclone separator by using a venturi, considering the venturi inlet width, total height of the cyclone, and body height of the cyclone. Laird and Albert (2002) made comparisons among different distributers in the vacuum tower and determined the twin-tangential circulation distributor as the best in terms of overall distribution performance. Zhou (2003) analyzed the energy dissipation of the twin-tangential annular flow gas distributor and determined that the size and curvature of the internal space of

Received on October 8, 2019; accepted on September 26, 2020
DOI: 10.1252/jcej.19we166
Correspondence concerning this article should be addressed to X. Xiao (E-mail address: xmxiao@tju.edu.cn).

the distributor were the most important factors affecting the pressure drop. Feng (2004) and Zhang (2004) investigated the partial structure parameters of a distributor by using the Euler–Lagrangian model. Liu *et al.* (2007) used a two-phase feed mode to investigate the entrainment of the mist in the distributor. Du (2005) further compared the gas distribution of single and two-phase feeds and found that the uniformity of distribution showed a slight change, while the pressure drop was modified significantly.

However, limited studies have been conducted on determining the mathematical relationship between the mal distribution or pressure drop and the geometric parameters of a distributor; this is very important for the industrial design of distributors. Some scholars studied the mathematical relationship between the other tower internals and pressure drop or mal distribution. Based on an approximate solution to the liquid and vapor transport equations within the packing, Edwards *et al.* (1999) defined the mal distribution depth of penetration (l_m) to characterize the mal distribution of the tower. Darakchiev and Dodev (2002) stated that every packing has its own nonuniformity and could be used for determining the penetration depth. Billingham and Lockett (2002) adopted the maximum mal distribution (f_{max}) to assess the sensitivity of a packed bed to mal distribution. Petrova *et al.* (2003) divided the column into several sections and the redistribution capability of each section was characterized by the dimensionless height of the tower. Wehrli *et al.* (2003) assessed the uniformity of the flow in the standard inlet below the packing by using coefficient of variation K_p based on three geometrical parameters. Luo *et al.* (2008) analyzed the relationship between the pressure drop and channel-opening angle of the column containing structured packing. Said *et al.* (2011) studied the impact of packing geometry variations on the dry pressure drop and determined a correlation between the pressure drop and changes in the packing geometry. Rafati Saleh *et al.* (2011) studied the effects of the bends on the pressure drop of structured packing by using the baseline k–ε (BSL) model.

In the present study, the mal distribution factor (*MF*) and pressure drop (ΔP) of a two-direction vapor horn gas distributor were simulated by using a 3D computer model code. More detailed parameters of the distributor were analyzed, including the distance between the inner sleeve and tower wall (H), height of the inner sleeve (h), height of the first vane (h'), radial slope angle (θ), number of vanes (N), and feed velocity (v), were analyzed to determine their effects on the gas distribution and pressure drop. A series of orthogonal simulation experiments were conducted to establish the mathematical correlation of the structural parameters to the mal distribution factor and pressure drop in the exponential form.

1. Computational Fluid Dynamics Modeling

1.1 Governing equations

Navier–Stokes equations were considered as the general conservation equations describing the gas flow within a distributor. The continuity and momentum for the gas phase are formulated as follows:

Continuity equation:

$$\frac{\partial \rho}{\partial t} + \nabla(\rho U) = 0 \tag{1}$$

Momentum equation:

$$\frac{\Delta(\rho U)}{\Delta t} + \nabla(\rho UU) = -\nabla P + \nabla \tau + B \tag{2}$$

where ρ is the fluid density, U is the interstitial velocity, B is the body force, P is the pressure, and τ is the tension of the tensor.

Compared with the standard k–ε model, the RNG k–ε model considers the swirl and swirl flow in the mean flow by modifying the turbulent viscosity. The effective viscosity is computed using the high-Reynolds number form in Eqs. (3)–(5).

$$\mu_{\text{eff}} = \mu + \mu_{\text{t}} \tag{3}$$

$$\mu_{\text{t}} = \rho C_{\mu} \frac{k^2}{\varepsilon} \tag{4}$$

$$C_{\mu} = 0.0845 \tag{5}$$

where μ_{eff} is the effective viscosity, μ_{t} is the turbulence eddy viscosity, C_{μ} is the constant to compute eddy viscosity.

1.2 Simulated geometries and boundary conditions

In this study, the commercial software package, FLUENT version 15.0, combined with Gambit 2.4.6 was employed for the geometric modeling, grid generation, and calculation. The incompressible, isothermal flow and steady state conditions were assumed for the calculation of fluid flow in the column tower. By conducting a set of simulations to ensure that the solution is independent of the grid numbers, the numbers of grid cells were set as 1.1×10^7.

The two-direction vapor horn gas distributor is depicted in **Figure 1**, in which the gas after entering from the vapor inlet flows along the left and right tangential directions separately through guide vanes, is preliminarily distributed to the bottom of the tower through more vanes, and finally bends upward to be uniformly distributed, as shown in **Figure 2**.

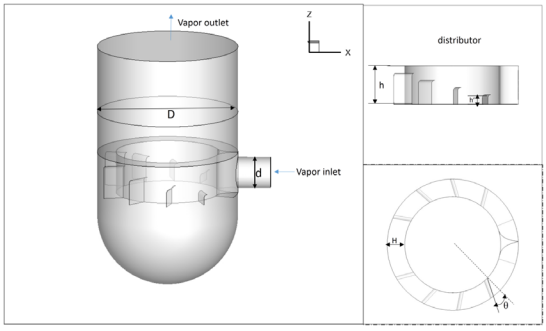

Fig. 1 Solution domain

The bottom of the packed column, especially the zones around the feed distributor, was considered as the calculation area. The gas distribution and pressure drop are affected by the following factors: the distance between the inner sleeve and tower wall (H), height of inner sleeve (h), height of the first vane (h'), radial slope angle (θ), number of vanes (N), diameter of the tower (D) and diameter of the inlet (d), as shown in Figure 1. As an important factors, the inlet velocity is also considered as a variable. Each factor was selected at five levels, as shown in **Table 1**.

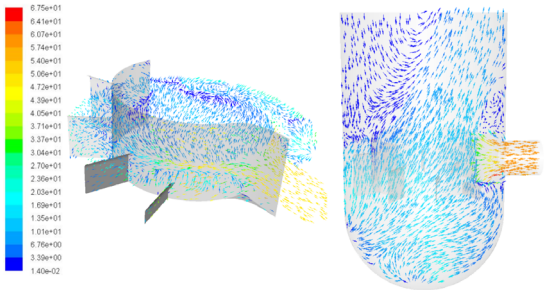

Fig. 2 Gas velocity vectors in the tower (m/s)

Table 1 Main parameters of the two direction vapor horn gas distributor

Levels	H [m]	H [m]	h' [m]	θ [°]	N	V [m·s^{-2}]
1	1.7	1.8	0.6	0	6	30
2	1.4	2.0	0.8	10	8	40
3	1.1	2.2	1.0	20	10	50
4	0.8	2.4	1.2	30	12	60
5	0.5	2.6	1.4	40	14	70

The orthogonal method was employed to organize the simulation program, as shown in **Table 2**.

To better guide the industrial design, the values of the geometric parameters and velocity were chosen to be equal to those of an industrial-grade packed tower. The diameter of the column is 8.2 m and the diameter of the gas feed nozzle is 1.8 m. The vapor flow was assumed to be incompressible, and it was measured by the real atmospheric feed and vacuum system: $\rho_{gas} = 0.317\,kg/m^3$ and $\mu_{gas} = 9.05\times10^{-6}$ pa·s. Temperature variations were neglected. The detailed boundaries and boundary conditions of the model are described in **Table 3**. The turbulence intensity is calculated as follows:

$$I = \frac{u'}{u_{avg}} = 0.16(Re)^{-1/8} \tag{6}$$

where u' is the turbulent velocity fluctuation and u_{avg} is the average velocity of turbulence.

The relative error between two successive iterations was specified using a convergence criterion of 10^{-4} for each scaled residual component. An Intel(R) Xeon(R) CPU running on 8-core 2.30 GHz with 64 GB of RAM was used to perform the simulations.

1.3 Evaluation method

The mal distribution factor (MF), which represents the ability of the distributing device to equalize the gas flow, was used to quantify the uniformity of the gas–velocity parameter. The MF is calculated at horizontal planes through the

Table 2 Simulation program

Experiment number	H/D	h/d	h'/d	θ/π	N	$(v_i-v_{min})/(v_{max}-v_{min})$
1	0.207	1.000	0.333	0.000	4.000	0.000
2	0.207	1.111	0.444	0.056	6.000	0.250
3	0.207	1.222	0.556	0.111	8.000	0.500
4	0.207	1.333	0.667	0.167	10.000	0.750
5	0.207	1.444	0.778	0.222	12.000	1.000
6	0.171	1.000	0.444	0.111	10.000	1.000
7	0.171	1.111	0.556	0.167	12.000	0.000
8	0.171	1.222	0.667	0.222	4.000	0.250
9	0.171	1.333	0.778	0.000	6.000	0.500
10	0.171	1.444	0.333	0.056	8.000	0.750
11	0.134	1.000	0.556	0.222	6.000	0.750
12	0.134	1.111	0.667	0.000	8.000	1.000
13	0.134	1.222	0.778	0.056	10.000	0.000
14	0.134	1.333	0.333	0.111	12.000	0.250
15	0.134	1.444	0.444	0.167	4.000	0.500
16	0.098	1.000	0.667	0.056	12.000	0.500
17	0.098	1.111	0.778	0.111	4.000	0.750
18	0.098	1.222	0.333	0.167	6.000	1.000
19	0.098	1.333	0.444	0.222	8.000	0.000
20	0.098	1.444	0.556	0.000	10.000	0.500
21	0.061	1.000	0.778	0.167	8.000	0.250
22	0.061	1.111	0.333	0.222	10.000	0.500
23	0.061	1.222	0.444	0.000	12.000	0.750
24	0.061	1.333	0.556	0.056	4.000	1.000
25	0.061	1.444	0.667	0.111	6.000	0.000

Table 3 Boundary conditions

Boundary	Boundary condition	Addition
Vapor inlet	Velocity-inlet	Uniform velocity profile, Intensity and hydraulic diameter
Vapor outlet	Pressure-outlet	Intensity and hydraulic diameter
Distributor	Wall	Stationary wall
Tower	Wall	Stationary wall

column as follows:

$$MF = \sqrt{\frac{1}{n}\sum_{i=1}^{n}\left(\frac{v_i - v_0}{v_0}\right)^2} \tag{7}$$

where v_i is the gas velocity in cell i (local velocity), v_0 is the superficial gas velocity, and n is the total number of measurement cells. A uniform distribution or plug flow can be reached when MF approaches zero. With the increase in MF, the distribution of gas flow in the packed bed becomes less uniform.

As MF is based on the superficial velocity, its value for the gas-velocity component in the z direction (MF_z) is also calculated to better indicate the impact in terms of velocity. When gas passes through the distributor, the speed component in the z direction plays a decisive role (Zeng *et al.*, 2009).

Pressure drop, which expresses energy consumed when gas flows through distributor, is calculated as:

$$\Delta P = P_{\text{in}} - P_{\text{out}} \tag{8}$$

where, P_{in} and P_{out} are the pressures of the vapor inlet and outlet, respectively.

1.4 Model verification

Experimental evidence is required to verify the numerical approach in Section 2.3. The data reported here were collected by (Zhang *et al.*, 2001; Liu *et al.*, 2007). In their experiments, the diameter of the column was 1 m with a height of 1.5 m, and the diameter of the gas feed nozzle was 0.15 m. The spacing between the inner vertical cylindrical wall and tower wall was 0.15 m, and eight flow vanes with radial slope angle of 0° were installed in the distributor. For model verification, a numerical simulation was performed by adopting a distributor with a size identical to that used in the experiment using the above-mentioned CFD calculation model. The simulation results of the dry pressure drop compared with the experimental results are shown in **Figure 3**. As shown, the simulation results show good consistency with the experimental results. Therefore, the numerical calculation model can be judged to be reasonable and credible.

2. Results and Discussion

2.1 Influence on the gas distribution for a single factor

2.1.1 Distance between the inner sleeve and tower wall (H) As shown in **Figure 4**, the pressure drop decreases with an increase in H, and the MF and MF_z increase.

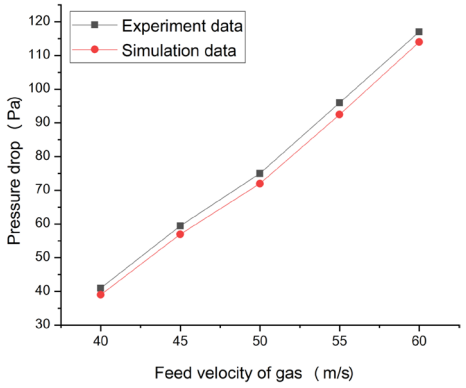

Fig. 3 ΔP at different gas feed velocities

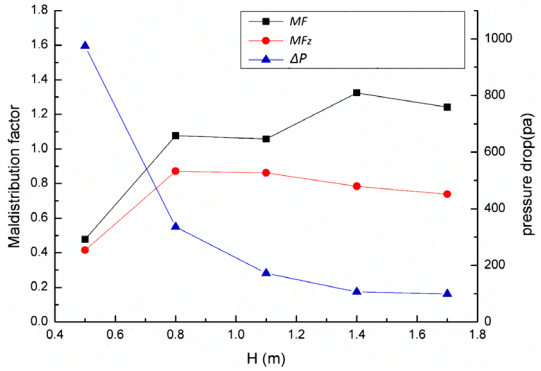

Fig. 4 MF, MF_z, ΔP at different values of H (h = 2.2 m, h' = 1.0 m, θ = 20°, N = 8, and v = 50 m/s)

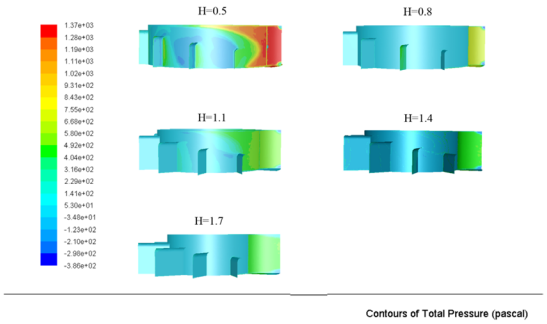

Fig. 5 Total pressure at the distributor with varying H (h = 2.2 m, h' = 1.0 m, θ = 20°, N = 8, and v = 50 m/s)

Besides, the deviation of MF and MF_z increase with the increase in H. When the H is small, the gas flows into the distributor through a relatively small area, and the increase of the local gas velocity would result in a greater loss of pressure due to internal friction, as shown in **Figure 5**. In addition, for a small value of H, the gas guided by the vanes is easily flows in the vertical and horizontal directions and achieves better distribution, as shown in **Figure 6**. In fact, H also affects the position of the high-speed region. With the increase in H, the high-speed zone tends to move toward the center of the tower, presenting a better symmetry, as shown in **Figure 7**.

2.1.2 Height of the inner sleeve (h) As shown in **Figure 8**, the value of ΔP as well as those of MF and MF_z de-

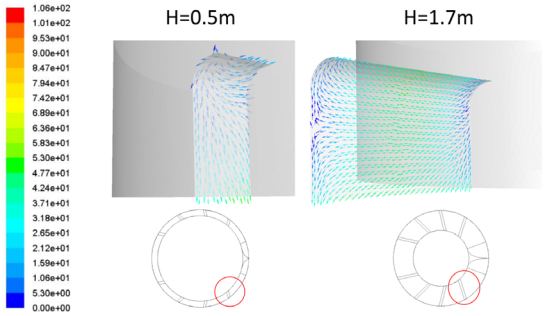

Fig. 6 Investigation of the effects on the gas vector for different values of H

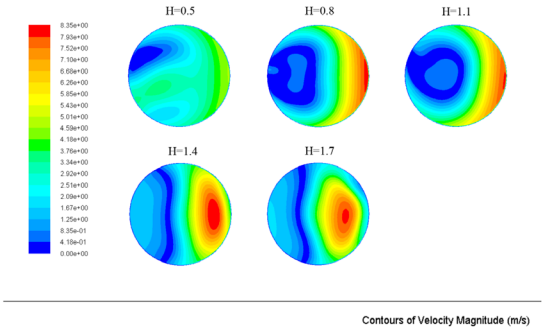

Fig. 7 Velocity profiles at the cross-section of the vapor outlet with varying H ($h=2.2$ m, $h'=1.0$ m, $\theta=20°$, $N=8$, and $v=50$ m/s)

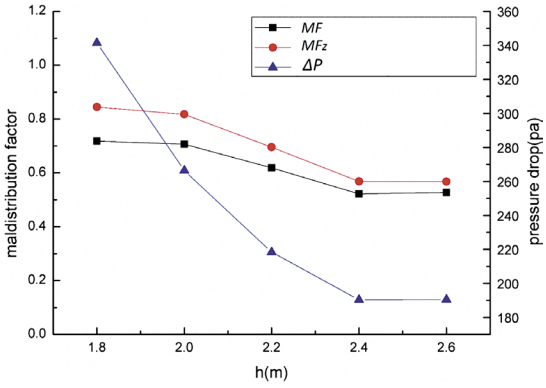

Fig. 8 MF, MF_z, and ΔP at different values of h ($H=1.1$ m, $h'=1.0$ m, $\theta=40°$, $N=8$, and $v=60$ m/s)

crease with the increase of h, and when h increases to a certain extent, the decrease tendency of MF and MF_z reduces. The change of h also changes the size of the annular channel, resulting in the change of ΔP, MF, and MF_z. For a small inner sleeve height (h), the local velocity is reduced and the turbulent kinetic-energy dissipation decreases; these phenomena are conducive to the decrease of ΔP, as illustrated in **Figure 9**. Further, as shown in **Figure 10**, the high-speed zone at the outlet does not shift and the velocity distribution becomes homogeneous.

2.1.3 Height of first vane (h') Since the height of vanes is increased in an arithmetic sequence, when fixing the vane number and height of the last vane, the height of the first vane becomes the key point of the vane design. As shown in

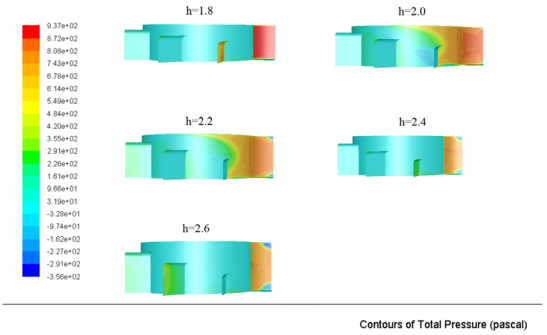

Fig. 9 Total pressure at the distributor with varying h ($H=1.1$ m, $h'=1.0$ m, $\theta=40°$, $N=8$, and $v=60$ m/s)

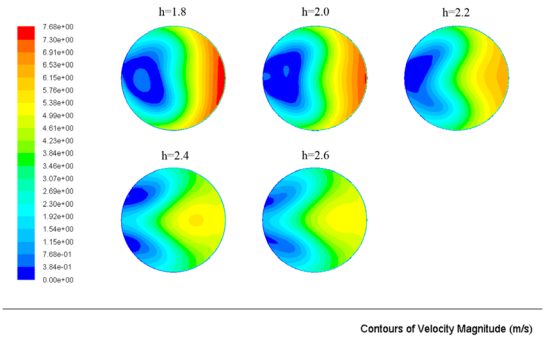

Fig. 10 Velocity profiles at the cross-section of the vapor outlet with varying h ($H=1.1$ m, $h'=1.0$ m, $\theta=40°$, $N=8$, and $v=60$ m/s)

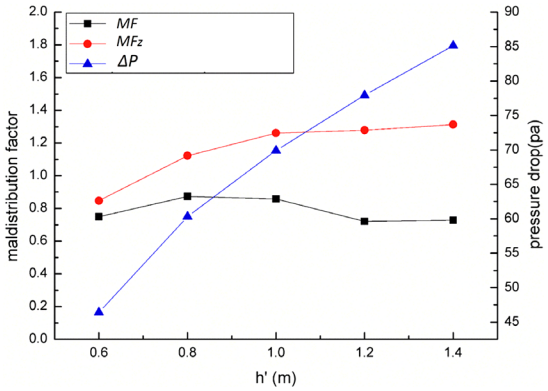

Fig. 11 MF, MF_z, and ΔP at different values of h' ($H=1.1$ m, $h=2.2$ m, $\theta=10°$, $N=10$, and $v=30$ m/s)

Figure 11, both MF and MF_z increases with the increase in h'. When h' reaches 1 m, MF_z changes slightly, and MF first reduces slightly and then remains constant. When the gas reaches the top of the vane, a phenomenon occurs similar to the boundary-layer separation. An interface exists between the main fluid and reflux fluid. When the height of the first vane is increased to a certain value, as shown in **Figure 12**, the gas reflux zone beneath the interface will cover the rear vanes, rendering the other vanes ineffective and MF remains almost unchanged. The pressure drop of the distributor increases with increasing of h'. The pressure changes through the distributor are shown in **Figure 13**; as shown, the big pressure drop mainly occurs before the first vane. As shown in **Figure**

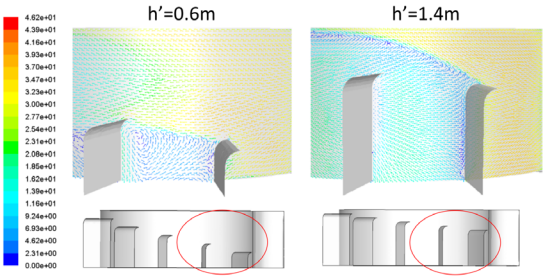

Fig. 12 Investigation of the effects on the gas vector for different values of h'

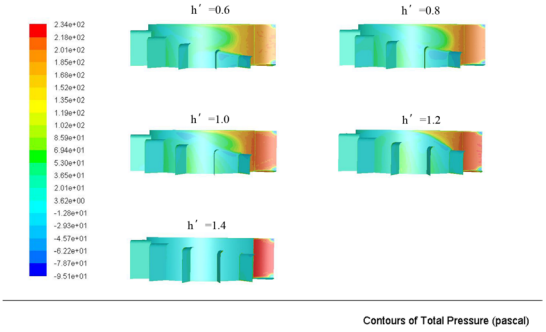

Fig. 13 Total pressure at distributor with varying h' ($H=1.1$ m, $h=2.2$ m, $\theta=10°$, $N=10$, and $v=30$ m/s)

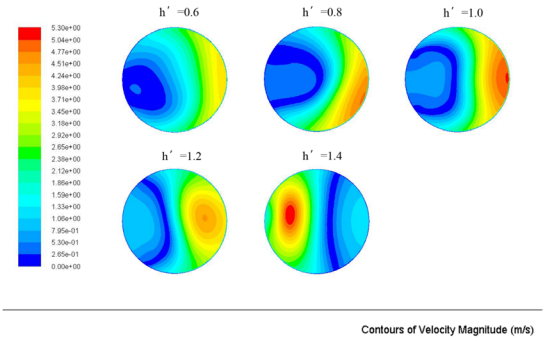

Fig. 14 Velocity profiles at the cross-section of the vapor outlet with varying h' ($H=1.1$ m, $h=2.2$ m, $\theta=10°$, $N=10$, and $v=30$ m/s)

14, h' has a great influence on the distribution of gas high-speed region. With the increase of h', the high-speed zone gradually moves from one end of the tower wall to the other. This is mainly due to the change in h' seriously affecting the amount of gas passing between the neighboring vanes.

2.1.4 Radial slope angle (θ) As shown in **Figure 15**, ΔP decreases with the increase of θ, while MF and MF_z first decreases, reach their minimum of $\theta=20°$, and then increase. In the case of gas distribution, the vane with a certain radial angle could help the fluid flow reach the center of turbulence that is not close to the wall of the tower; that in turn facilitates the fluid in the tower to distribute evenly. In the case of pressure drop, the vane with a larger value of θ has a better guidance toward the fluid flow, resulting in a steady decline of pressure through the annular channel, and illustrated in **Figure 16**. As shown in **Figure 17**, with the increase of θ, the high-speed zone moves from the tower wall to the center and then returns to the tower wall.

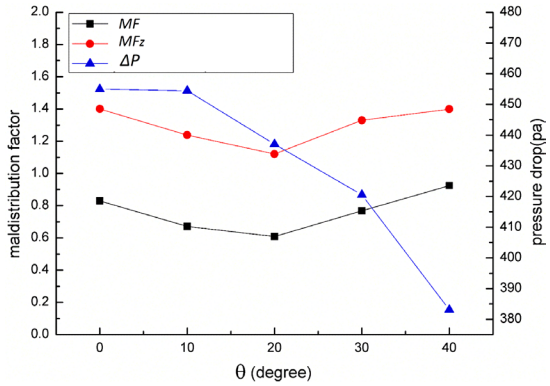

Fig. 15 MF, MF_z, and ΔP at different values of θ ($H=1.1$ m, $h=2.0$ m, $h'=1.2$ m, $N=10$, and $v=70$ m/s)

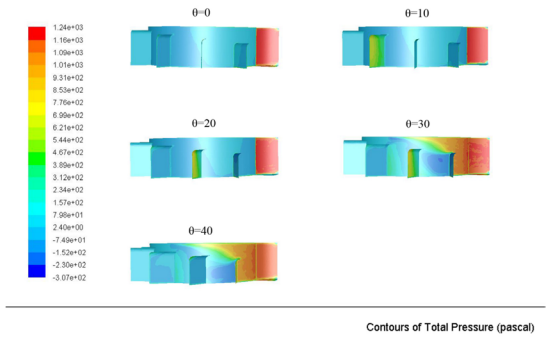

Fig. 16 Total pressure at distributor with varying θ ($H=1.1$ m, $h=2.0$ m, $h'=1.2$ m, $N=10$, and $v=70$ m/s)

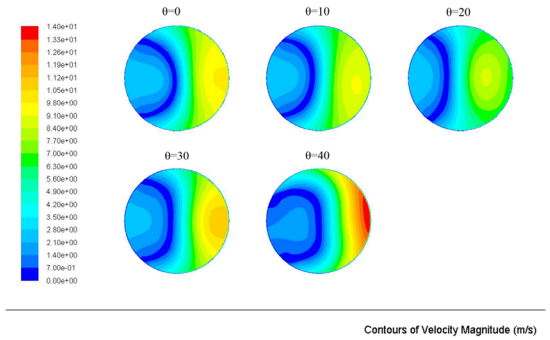

Fig. 17 Velocity profiles at the cross-section of the vapor outlet with varying θ ($H=1.1$ m, $h=2.0$ m, $h'=1.2$ m, $N=10$, and $v=70$ m/s)

2.1.5 Number of vanes (N) As shown in **Figure 18**, with the increase of N, both the MF and MF_z gradually reduces, and this suggests that the more the number of vanes, the more evenly the gas is dispersed to achieve a better distribution. The minimum pressure drop occurs at point $N=4$, increases abruptly, and then decreases gradually. This is because when the number of vanes is very small ($N=4$), the gas can pass through the annular channel, almost unimpeded, with relatively small local velocity, as shown in **Figure 19**, and the gas is almost free of the vortex, as shown in **Figure 20**. Vortexes are evidently generated with $N=6$, and

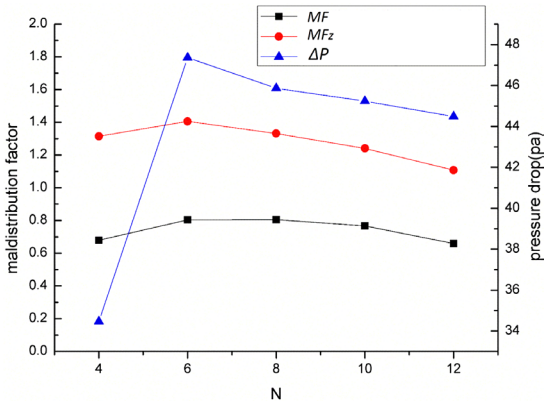

Fig. 18 MF, MF_z, and ΔP at different values of N ($H = 1.1$ m, $h = 2.0$ m, $h' = 1.2$ m, $\theta = 10°$, and $v = 70$ m/s)

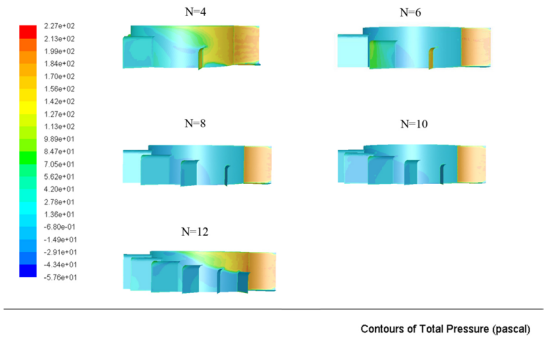

Fig. 19 Total pressure at the distributor with varying N ($H = 1.1$ m, $h = 2.0$ m, $h' = 1.2$ m, $\theta = 10°$, and $v = 70$ m/s)

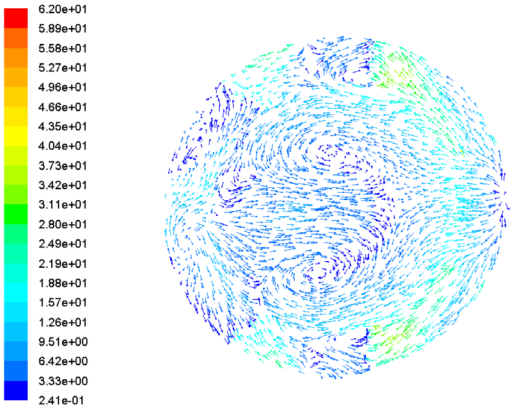

Fig. 20 Velocity vectors for vanes number at $N = 4$ (m/s)

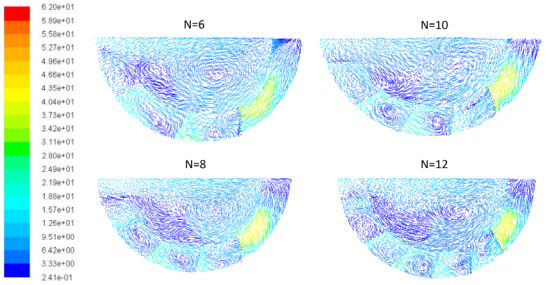

Fig. 21 Velocity vectors for vanes number at $N = 6$, 8, 10, and 12 (m/s)

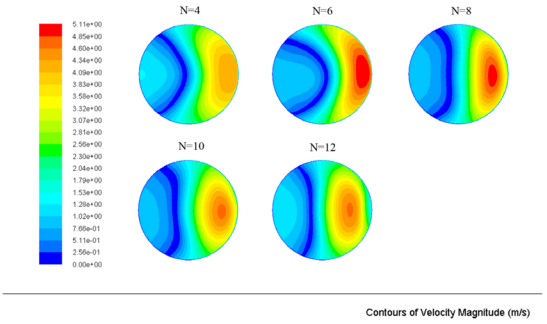

Fig. 22 Velocity profiles at the cross-section of the vapor outlet with varying N ($H = 1.1$ m, $h = 2.0$ m, $h' = 1.2$ m, $\theta = 10°$, and $v = 70$ m/s)

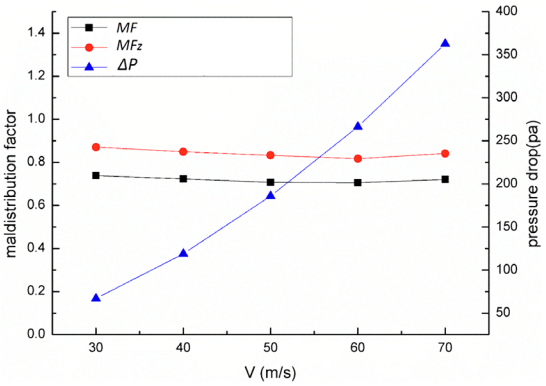

Fig. 23 MF, MF_z, and ΔP at different v ($H = 1.1$ m, $h = 1.8$ m, $h' = 1.0$ m, $N = 6$, and $\theta = 40°$)

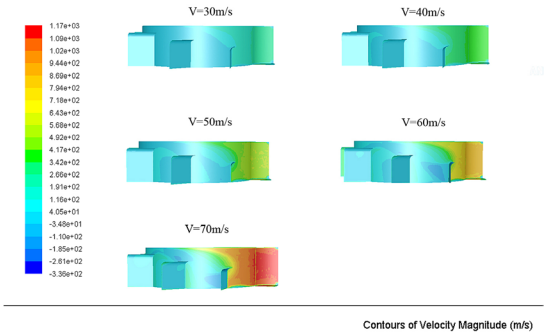

Fig. 24 Total pressure at the distributor with varying v ($H = 1.1$ m, $h = 1.8$ m, $h' = 1.0$ m, $N = 6$, and $\theta = 40°$)

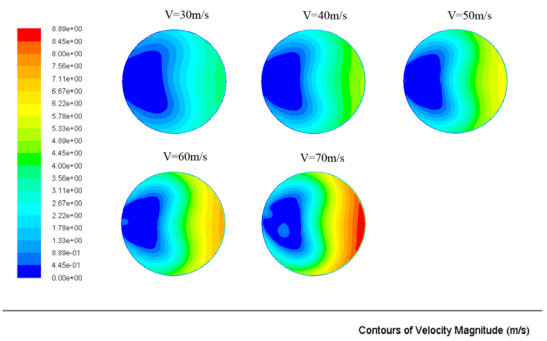

Fig. 25 Velocity profiles at the cross-section of the vapor outlet with varying v ($H = 1.1$ m, $h = 1.8$ m, $h' = 1.0$ m, $N = 6$, and $\theta = 40°$)

with the increase of N, the large vortexes could be divided into small ones, as shown in **Figure 21**. This reduces the collision friction among the gas flows, and the pressure drop is reduced with the increase in the number of vanes. Furthermore, N can adjust the position of the high-speed zone, as shown in **Figure 22**.

2.1.6 Feed velocity **Figures 23–25** show that with the increase in the inlet gas velocity, the pressure drop of the distributor increases. Moreover, with the speed 30–70 m/s, MF and MF_z remains relatively stable; this is consistent with the study of (Liu *et al.*, 2007).

2.2 Fitting of *MF* and pressure drop formula

For a given two-direction vapor horn gas distributor, ΔP and MF are obtained from a range of geometrical and physical parameters, including the diameter of the column (D), inlet diameter (d), distance between the inner sleeve and tower wall (H), height of the inner sleeve (h), height of the first vane (h'), radial slope angle (θ), number of vanes (N), and inlet velocity in the column (v).

At present, in the design of the distributor, the main method to obtain the MF and ΔP involves conducting experimental measurements or simulations of the designed distributor. However, in engineering design, operating conditions are obtained first, i.e., acceptable values of pressure drop and uneven distribution of gas are determined. Thus, a simple correlation must be established between the geometrical parameters of the distributor and MF as well as ΔP. In this study, we propose two empirical correlation equations. The form of the empirical correlation equation was modeled as an exponential product formula, as the expression is simple and can cover variations of every variable. By referring to the correlation equation proposed by (Stichlmair and Mersmann, 1978) based on the drag coefficient model, the equation can be formulated as follows:

$$\frac{\Delta P}{P_s} = a_0 \frac{\rho_{gas}}{\rho_s}\left(\frac{H}{D}\right)^{a_1}\left(\frac{h}{d}\right)^{a_2}\left(\frac{h'}{d}\right)^{a_3}\left(\frac{\theta}{\pi}+1\right)^{a_4}(N)^{a_5} \times\left(\frac{v-v_{min}}{v_{max}-v_{min}}+1\right)^{a_6} \quad (9)$$

$$\Delta P = a_0 P_s \frac{\rho_{gas}}{\rho_s}\left(\frac{H}{D}\right)^{a_1}\left(\frac{h}{d}\right)^{a_2}\left(\frac{h'}{d}\right)^{a_3}\left(\frac{\theta}{\pi}+1\right)^{a_4}(N)^{a_5} \times\left(\frac{v-v_{min}}{v_{max}-v_{min}}+1\right)^{a_6} \quad (10)$$

$$L = a_0 P_s \frac{\rho_{gas}}{\rho_s} \quad (11)$$

In Eqs (9)–(11), a_0, $a_1 \ldots a_6$ represent the constant parameters, P_s is the standard atmospheric pressure, ρ_s is the standard air density, and v_{min} and v_{max} are the maximum and minimum velocities at the inlet, respectively, with $v_{min} = 30$ m/s and $v_{max} = 70$ m/s.

For both sides of the equation, a logarithmic equation can be simultaneously obtained as follows:

$$\ln\Delta P = \ln a_0 P_s \frac{\rho_{gas}}{\rho_s} + a_1 \ln\left(\frac{H}{D}\right) + a_2 \ln\left(\frac{h}{d}\right) + a_3 \ln\left(\frac{h'}{d}\right) + a_4 \ln\left(\frac{\theta}{\pi}+1\right) + a_5 \ln N + a_6 \ln\left(\frac{v-v_{min}}{v_{max}-v_{min}}+1\right) \quad (12)$$

The mean square error of the fitting function with the simulation data can be expressed as:

$$Q(a_0, a_1, a_2, a_3, a_4, a_5, a_6) = \sum_{i=0}^{n} (\ln \Delta P_i - y_i)^2 \quad (13)$$

The minimal value of the $Q(a_0, a_1, a_2, a_3, a_4, a_5, a_6)$ satisfies

$$\frac{\partial Q}{\partial a_i} = 0 \quad (14)$$

where, $i = 0, 1 \ldots 6$.

The parameter values thus obtained as follows: $a_0 = 5.691 \times 10^{-5}$, $a_1 = -1.985$, $a_2 = -1.92$, $a_3 = 0.5333$, $a_4 = -0.7010$, $a_5 = 0.3381$, and $a_6 = 2.420$. The simulation results obtained the range of the investigated formula used to establish the ΔP. The mean deviation between ΔP predicted from the empirical formula and the corresponding values calculated from the simulated CFD results was approximately 16% and the maximum deviation was 26%. The discrepancy between the corresponding value of ΔP is observed in the parity plot of **Figure 26**. Similarly, the expression of MF was also obtained, as described in equation 15. The parameter values obtained included $b_0 = 0.5771$, $b_1 = 0.0396$, $b_2 = -0.2897$, $b_3 = 0.3480$, $b_4 = -0.5270$, $b_5 = 0.2062$, and $b_6 = 0.3113$. The mean deviation between the MF predicted from the empirical formula and the corresponding values calculated from the simulated CFD results was approximately 7.4% and the maximum deviation was 24%. The discrepancy between the corresponding MF is shown in **Figure 27**. Furthermore, by substituting the structural parameters of the control experiment into the empirical formula, we obtained the deviation of ΔP and MF as 7.5% and 3.1%, respectively, at the speed of 40 m/s.

$$MF = b_0\left(\frac{H}{D}\right)^{b_1}\left(\frac{h}{d}\right)^{b_2}\left(\frac{h'}{d}\right)^{b_3}\left(\frac{\theta}{\pi}+1\right)^{b_4}(N)^{b_5} \times\left(\frac{v-v_{min}}{v_{max}-v_{min}}+1\right)^{b_6} \quad (15)$$

In the design of the distributor, geometric-parameters optimization is essential. However, it is difficult to know the exact performance variation with parameter change. In particular, in the atmospheric and vacuum systems, a balance is necessary between the pressure drop and unevenness of the gas. By using the aforementioned formulas, MF and ΔP in the gas distributor can be quantitatively described with several geometric parameters of the same type distributor at a similar scale.

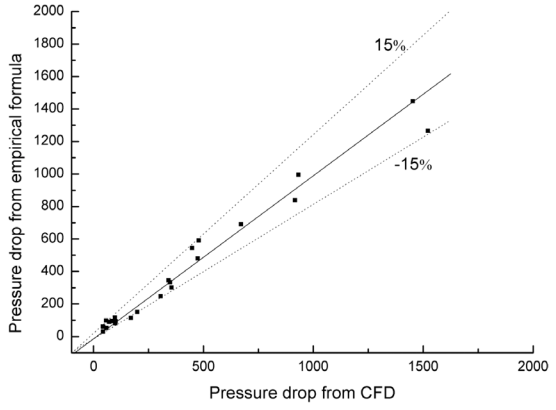

Fig. 26 Correlation between predicted and simulated pressure drop values (Pa)

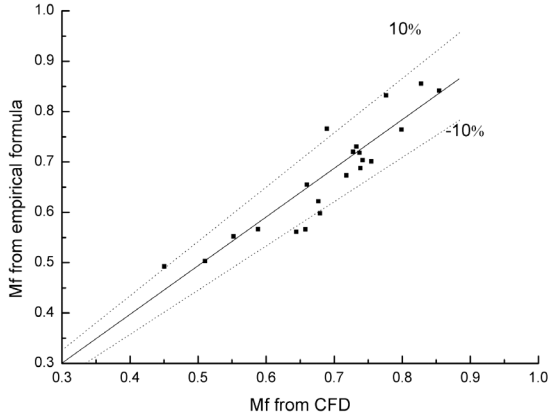

Fig. 27 Correlation between predicted and simulated mal distribution factor values

Conclusion

In this paper, all of the key geometric parameters of two-direction vapor horn gas distributor were systematically investigated using the CFD method. The results showed that the main factor influencing the pressure drop was the space size at the inlet of the distributor. The parameters of the distance between the inner sleeve and tower wall, height of the first vane, and number of vanes had remarkable effects on the location of the high-speed zone of gas. Furthermore, we proposed a method for quantitatively describing *MF* and ΔP according to the geometric parameters of the two-direction vapor horn distributor and the operating parameters. A set of data was simulated through an orthogonal method, and two empirical correlation equations were obtained by analyzing each structural parameter of the industrial scale distributor. The deviation between the values was analyzed by comparing the simulation data and empirical formula. As such, the deviations in the *MF* and ΔP were obtained as approximately 7.4% and 16%, respectively.

Acknowledgement

We are grateful for the financial support from National Key R&D Program of China (No. 2017YFB0602702-02).

Nomenclature

a	=	coefficient of ΔP	[—]
B	=	body force	[—]
b	=	coefficient of M_f	[—]
C_μ	=	constant to compute Eddy viscosity	[—]
D	=	diameter of the tower	[m]
d	=	diameter of the inlet	[m]
H	=	distance between the inner sleeve and tower wall	[m]
h	=	height of the inner sleeve	[m]
h'	=	height of the first vane	[m]
I	=	turbulence intensity	[—]
K	=	turbulent kinetic energy	[$m^2 \cdot s^{-2}$]
L	=	coefficient of pressure drop equation	[Pa]
MF	=	mal distribution factor	[—]
MF_z	=	mal distribution factor for vertical velocity	[—]
N	=	number of vanes	[—]
P_{in}	=	pressure of the vapor inlet	[Pa]
P_{out}	=	pressure of the vapor outlet	[Pa]
Q	=	mean square error of fitting function	[—]
Re	=	Reynolds number	[—]
t	=	time	[s]
v	=	interstitial velocity	[$m \cdot s^{-1}$]
v_i	=	gas velocity in cell i	[—]
v_0	=	superficial gas velocity	[$m \cdot s^{-1}$]

‹Greek letters›

ΔP	=	pressure drop	[Pa]
ε	=	turbulence Eddy dissipation	[$m^2 \cdot s^{-3}$]
θ	=	radial slope angle	[°]
μ	=	viscosity	[Pa·s]
μ_{eff}	=	effective viscosity	[Pa·s]
μ_t	=	turbulence Eddy viscosity	[Pa·s]
ρ	=	density	[$kg \cdot m^{-3}$]
τ	=	tension tensor	[$kg \cdot m \cdot s^{-2}$]

Literature Cited

Billingham, J. F. and M. J. Lockett; "A Simple Method to Assess the Sensitivity of Packed Distillation Columns to Maldistribution," *Chem. Eng. Res. Des.*, **80**, 373–382 (2002)

Darakchiev, R. and C. Dodev; "Gas Flow Distribution in Packed Columns," *Chem. Eng. Process.*, **41**, 385–393 (2002)

Dhotre, M. and J. Joshi; "Design of a Gas distributor: Three-Dimensional CFD Simulation of a Coupled System Consisting of a Gas Chamber and a Bubble Column," *Chem. Eng. J.*, **125**, 149–163 (2007)

Du, Y.; Computational Fluid Dynamics (CFD) Study on Liquid–Gas Two Phase in Feed Distributor, Master Thesis, Tianjin Univercity, China (2005)

Edwards, D. P., K. R. Krishnamurthy and R. W. Potthoff; "Development of an Improved Method to Quantify Maldistribution and Its Effect on Structured Packing Column Performance," *Chem. Eng. Res. Des.*, **77**, 656–662 (1999)

Feng, C.; Study on Performance and Scale-Up Rule of Twin-Tangential Annular Flow Gas Distributor, Master Thesis, Tianjin Univercity, China (2004)

Haghshenasfard, M., M. Zivdar, R. Rahimi and M. Nasr Esfahany; "CFD Simulation of Gas Distribution Performance of Gas Inlet Systems in Packed Columns," *Chem. Eng. Technol.*, **30**, 1176–1180

(2007)
Laird, D. and B. Albert; "Optimization of Packed Tower Inlet Design by CFD Analysis," AIChE Spring National Meeting, New Orleans, U.S.A. (2002)
Liu, D., X. Li, S. Xu and H. Li; "CFD Simulation of Gas–Liquid Performance in Two Direction Vapour Horn," *Chem. Eng. Res. Des.*, **85**, 1375–1383 (2007)
Luo, S. J., W. Y. Fei, X. Y. Song and H. Z. Li; "Effect of Channel Opening Angle on the Performance of Structured Packings," *Chem. Eng. J.*, **144**, 227–234 (2008)
Muir, L. A. and C. L. Briens; "Low Pressure Drop Gas Distributors for Packed Distcllation Columns," *Can. J. Chem. Eng.*, **64**, 1027–1032 (1986)
Petrova, T., K. Semkov and C. Dodev; "Mathematical Modeling of Gas Distribution in Packed Columns," *Chem. Eng. Process.*, **42**, 931–937 (2003)
Said, W., M. Nemer and D. Clodic; "Modeling of Dry Pressure Drop for Fully Developed Gas Flow in Structured Packing Using CFD Simulations," *Chem. Eng. Sci.*, **66**, 2107–2117 (2011)
Rafati Saleh, A., S. H. Hosseini, S. Shojaee and G. Ahmadi; "CFD Studies of Pressure Drop and Increasing Capacity in MellapakPlus 752. Y Structured Packing," *Chem. Eng. Technol.*, **34**, 1402–1412 (2011)
Stichlmair, J. and A. Mersmann; "Dimensioning Plate Colunms for Absorption and Rectification," *Int. Chem. Eng.*, **18**, 223–236 (1978)
Venkatesh, S., M. Sakthivel, M. Avinasilingam, S. Gopalsamy, E. Arulkumar and H. P. Devarajan; "Optimization and Experimental Investigation in Bottom Inlet Cyclone Separator for Performance Analysis," *Korean J. Chem. Eng.*, **36**, 929–941 (2019)
Wehrli, M., S. Hirschberg and R. Schweizer; "Influence of Vapour Feed Design on the Flow Distribution Below Packings," *Chem. Eng. Res. Des.*, **81**, 116–121 (2003)
Zeng, J., A. Gan, S. Ma and X. Li; "Study on Two-Line Vane Gas Distributor," *Shiyou Huagong Sheji*, **26**, 16–18 (2009)
Zhang, L., B. Jiang and X. Li; "Size Distributions and Model of Droplets Motion on AR Gas Distributor," *Huagong Jinzhan*, **20**, 49–51 (2001)
Zhang, W.; Computational Fluid Dynamics on Vapor–Liquid Distributor in Large-Scale Packed Column and Optimum Design, Master Thesis, Tianjin Univercity, China (2004)
Zhou, H.; Study on Hydrodynamic Performance of Gas–Liquid Distributor in Large Packed Tower, Master Thesis, Tianjin Univercity, China (2003)